Experimental observation of superdiffusive transport in random dimer lattices

U Naether[1,5], **S Stützer**[2,5], **R A Vicencio**[1], **M I Molina**[1], **A Tünnermann**[2], **S Nolte**[2], **T Kottos**[3], **D N Christodoulides**[4] **and A Szameit**[2,6]

[1] Departamento de Física, MSI-Nucleus on Advanced Optics, and Center for Optics and Photonics (CEFOP), Facultad de Ciencias, Universidad de Chile, Santiago, Chile
[2] Institute of Applied Physics, Abbe Center of Photonics, Friedrich-Schiller-Universität Jena, Max-Wien-Platz 1, D-07743 Jena, Germany
[3] Department of Physics, Wesleyan University, Middletown, CT 06459, USA
[4] CREOL, The College of Optics and Photonics, University of Central Florida, Orlando, FL 32816, USA
E-mail: alexander.szameit@uni-jena.de

Abstract. We experimentally observe anomalous wavepacket evolution in a realization of a one-dimensional finite binary Anderson model in the presence of short-range correlations. To this end, we employ weakly-coupled optical waveguides with propagation constants ε_1 and ε_2. The correlations enforce the creation of dimers, i.e. two adjacent waveguides with the same ε, randomly placed along the lattice. A transition from a ballistic to a superdiffusive wavepacket expansion and, eventually, to localization is observed as the contrast between the two propagation constants increases.

[5] Both authors contributed equally.

[6] Author to whom any correspondence should be addressed.

IOP Institute of Physics ◆ DEUTSCHE PHYSIKALISCHE GESELLSCHAFT

Contents

1. Introduction

The common belief that in one-dimensional (1D) lattices the presence of any amount of disorder leads to exponential localization of all the eigenstates has been around since the seminal work by Anderson [1]. It is well known that in random 1D systems one never encounters mobility edges; that is, energy thresholds separating localized (insulating) states from the extended (conducting) ones. As a result, one observes a complete halt of diffusion and a suppression of any wavepacket expansion—a process observed in numerous experiments spanning many area of physics, such as optics [2–9], matter waves [10, 11], and even sound waves [12]. In recent years, this popular view has been critically reexamined in a number of theoretical studies through counter-examples, where correlations in a disordered potential can facilitate wavepacket delocalization [13] and long-range transport (for a recent review see [14]). The prototypical case considered in these works was that of a random dimer model (RDM) [15–17] where (in the context of a tight-binding Hamiltonian) pairs of adjacent on-site energies (dimers) are assigned at random positions in the lattice, leading to two-site correlations in an otherwise random binary model. For finite samples and below a certain disorder threshold, a number of transparent states emerge, and their existence results in a diffusive and superdiffusive wavepacket evolution. Indirect experimental evidences of delocalized eigenstates in such short-range correlated systems were previously reported [18–20]. However, a direct experimental demonstration of (super-)diffusive transport in such systems still remains elusive.

In this article, we report the first direct experimental observation of a 1D localization–delocalization transition in finite binary Anderson lattices as a result of short-range correlations. Our experimental set-up utilizes an optical waveguide array [21, 22] as a model system consisting of two types of waveguides with propagation constants ε_1 and ε_2 which are coupled evanescently with a tunneling rate C. We show that if ε_1 (or ε_2) is assigned at random to pairs of dimer lattice elements (that is, two waveguides in succession), an initially localized beam or wavepacket can become delocalized. Specifically, our measurements reveal an anomalous superdiffusive wavepacket spreading (something that was observed so far only in 3D systems [23]) which is suppressed once the disorder contrast between dimers exceeds a critical value $\Delta \equiv |\varepsilon_1 - \varepsilon_2| > 2C$. The findings reported in this work might open up new possibilities for controlling the transport of light via potential correlations and may shed new light on the understanding of wavepacket evolution in other areas of physics (like ultracold atoms, where correlations in experimentally induced disorder appears naturally).
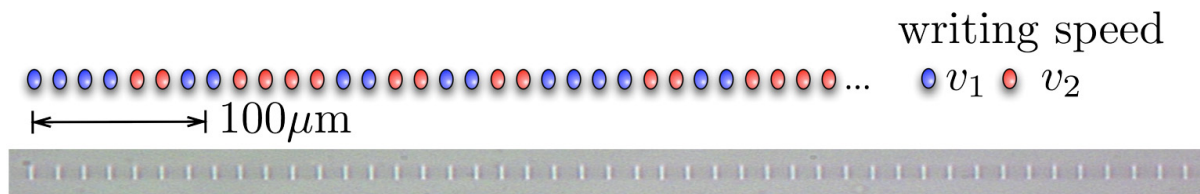
IOP Institute of Physics **Φ** DEUTSCHE PHYSIKALISCHE GESELLSCHAFT

Figure 1. Upper row: sketch of a random dimer array. Each dimer consists of two adjacent waveguides, where both waveguides exhibit the same propagation constant ε_1 or ε_2, that is assigned at random. Lower row: microscope image of a fabricated waveguide array.

2. The model

Our experimental setup, illustrated in figure 1, consists of a 1D waveguide array fabricated in fused silica, using the laser direct-writing technology [24]. The writing procedure is described in detail in [25]. The waveguides exhibit a binary distribution ε_1 or ε_2 of the waveguide propagation constants (compare the upper part of figure 1 for a sketch of a dimer realization) which appear in pairs of subsequent sites, with probability k and $1 - k$ respectively, where k is a random number in the interval [0,1]. Without loss of generality we consider the most disordered case, $k = 0.5$, for which

$$\varepsilon_{2n} = \varepsilon_{2n+1} = \begin{cases} \varepsilon_1 & \text{if} \quad \kappa \leqslant \frac{1}{2}, \\ \varepsilon_2 & \text{if} \quad \kappa > \frac{1}{2}. \end{cases} \tag{1}$$

The light evolution along the longitudinal z-axis in these weakly coupled single mode waveguides is described in general using a coupled mode theory approach. The associated equations are given by [21]

$$-\mathrm{i}\frac{\mathrm{d}a_n}{\mathrm{d}z} = \varepsilon_n a_n + C(a_{n+1} + a_{n-1}). \tag{2}$$

In the above equation $n = 1, \ldots, N$, where the even integer N represents the number of lattice sites (waveguides), a_n is the amplitude of the propagating optical field envelope in the nth waveguide, C is the coupling strength between nearest-neighbor lattice sites, and z is the longitudinal space coordinate. Equation (2) is effectively identical to the quantum description of non-interacting electrons in a solid crystal in the tight-binding approximation, provided that the role of the time variable t is now played by the propagation distance z. The advantage offered by our system is clearly the ability to directly observe the resulting wavefunction by measuring the distribution of light intensity during the propagation along the sample [26].

A useful quantity that defines the nature of the dynamical evolution of a wavepacket is the averaged variance of the intensity pattern as a function of z:

$$M(z) \equiv \left\langle \sum_n (n - n_0)^2 |a_n|^2 \right\rangle \sim z^\gamma, \tag{3}$$

where $\langle \cdots \rangle$ denotes an average over different disorder realizations (typically 100), and n_0 is the excited lattice site. The spreading exponent γ provides a quantitative description of the dynamics: $\gamma = 0$ corresponds to localization, $\gamma = 1$ to diffusion, $\gamma \in (1, 2)$ to superdiffusive motion and $\gamma = 2$ to ballistic motion.
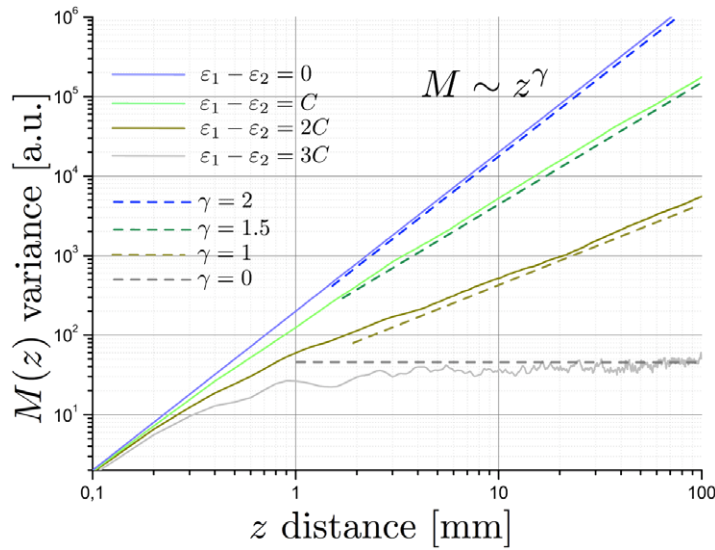
Figure 2. Theoretical plot of the variance of a propagating wavepacket for different detunings of the propagation constant between the two dimers. For $\gamma = 2$, one finds ballistic spreading, $\gamma = 1.5$ results in superdiffusive dynamics, $\gamma = 1$ corresponds to diffusive behavior and $\gamma = 0$ is the signature for Anderson localization.

We begin by simulating the beam evolution in this RDM array when only one site (δ_{n,n_0}) is initially excited—say at the center of the array. To this end, equation (2) has been integrated numerically using a self-expanding algorithm in order to eliminate finite-size effects. Our results for $M(z)$ for different values of the disorder contrast Δ are shown in figure 2. For $\Delta = 0$ (periodic lattice) the transport is ballistic resulting in a quadratic growth of the second moment, i.e.

$$M = \sum_n (n - n_0)^2 |J_{n-n_0}(2Cz)|^2 = 2C^2 z^2, \tag{4}$$

as expected for discrete diffraction [27]. Here, $J_n(x)$ is the Bessel function of the first kind. For $\Delta \neq 0$ we identify the following three regimes [15, 16]: for $0 < \Delta < 2C$ the motion is superdiffusive, i.e. $M(z) \propto z^{3/2}$,[7] while for $\Delta > 2C$ Anderson localization is observed, and the variance $M(z)$ saturates i.e. $M \propto$ constant. The transition point between superdiffusive transport and localization corresponds to $\Delta = 2C$ and is characterized by a diffusive spreading where $M(z) \propto z$.

The anomalous (super-)diffusive transport observed for $0 < \Delta \leqslant 2C$ is a new phenomenon induced via the short range correlations on the on-site potential (see equation (1)). At first glance, this result is very surprising because the RDM can be mapped to a random binary alloy with two atoms per unit cell. In this case, the ballistic transport of a photon is inhibited by wave interferences between the various paths where the particle is multiply scattered by disorder. The length-scale that dictates the transport is the so-called localization length ξ and it is usually associated with the inverse of the exponential decay rate of the eigenstates from some

---

[7] Of course in the asymptotic limit $z \to \infty$ the localized nature of the modes—apart from some resonances which in this limit have measure zero—will be revealed leading to saturation. However, for all practical purposes associated with finite samples this saturation is irrelevant and it will never be observed.

localization center. According to the standard theory of 1D localization [28] one expects that all modes are exponentially localized, which results in a vanishing spreading exponent $\gamma \to 0$.

The origin of the anomalous diffusion can be understood by considering the structural difference of the eigenmodes associated to the system described by equations (1), (2) and the standard random binary alloy due to the presence of short-range correlations in the disorder. As already mentioned above, in 1D *almost* all eigenstates, except for some isolated stochastic resonances (the so-called Azbel resonances) [29], are localized in infinitely large samples, regardless how weak the disorder is. Since the measure of these resonances is zero, and since they appear randomly in the energy spectrum for each disorder realization, they do not contribute to transport, and thus one observes a vanishing of the diffusion constant (proportional to conductance by the Einstein relation) and, therefore, inhibited transport. Moreover, the width $\mathrm{d}E$ of these Azbel resonances as a function of the energy of the incoming particle becomes exponentially small as the number of elements N of the system (or the strength of the disorder) increases, i.e. $\mathrm{d}E \sim \exp(-N/\xi)$.

In contrast to random binary lattices, in the case of the RDM it was found that short-range correlations in the disorder potential as given by equation (1) lead to fully transparent (resonant) states at energies $E_\mathrm{r} = \varepsilon_1$ and $E_\mathrm{r} = \varepsilon_2$. RDM resonances differ substantially from Azbel resonances since they appear for any realization of the random potential. Moreover, it was found that the nearby eigenstates with energies $E = E_\mathrm{r} \pm \delta$ have a diverging localization length $\xi(E_\mathrm{r} \pm \delta) \sim 1/\delta^2$ if $\Delta < 2C$ and $\xi(E_\mathrm{r} \pm \delta) \sim 1/\delta$ if $\Delta = 2C$ [30]. In the case $\Delta < 2C$ there exist $\sqrt{N}$ modes that appear *as if they are extended* for any finite sample of length $N < \xi(E_\mathrm{r} \pm \delta)$ and contribute to the spreading of an initial single-site excitation δ_{n,n_0} [30]. The associated diffusion constant can be calculated through the Boltzmann relation $D(E) = v(E)\xi(E)$, as the energy intergral of $D(E)$, where the integration will be over the energy interval $E_\mathrm{r} \pm \delta$ which supports the $\sqrt{N}$ 'extended' states that participate in the transport. Note that in the Boltzmann relation we have substituted the mean free path with the localization length $\xi(E)$ as these two characteristic lengths are approximately equal in the 1D case. Furthermore, assuming that the transport velocity is approximately constant $v(E) = v$ in this energy window, we find that

$$D_\mathrm{tot} = \int D(E)\,\mathrm{d}E \sim v\delta\,\xi(E). \tag{5}$$

Substitution of the expression for $\xi(E)$ near the resonance energies leads to

$$D_\mathrm{tot} \sim v/\delta \quad \text{for} \quad \Delta < 2\mathrm{C}, \tag{6}$$

$$D_\mathrm{tot} \sim v \quad \text{for} \quad \Delta = 2\mathrm{C}. \tag{7}$$

For the case $\Delta = 2C$, equation (7) immediately results in $M(z) \sim D_\mathrm{tot}z \sim z$. In order to analyze the case $\Delta < 2C$ one needs to recall that the number of modes which are extended over the whole system of size N is $\sqrt{N} \sim \sqrt{\xi} \sim 1/\delta$. Substituting the latter expression in equation (6) we get

$$D_\mathrm{tot} \sim v\sqrt{N} \sim v\sqrt{z}. \tag{8}$$

Here we assume again that the extended states traverse the system with constant velocity and thus the 'time' z and the system size N can be interchanged. Consequently for $\Delta < 2C$, the mean square displacement grows as $M(z) \sim z^{3/2}$. The above heuristic arguments are nicely confirmed by simulations shown in figure 2.
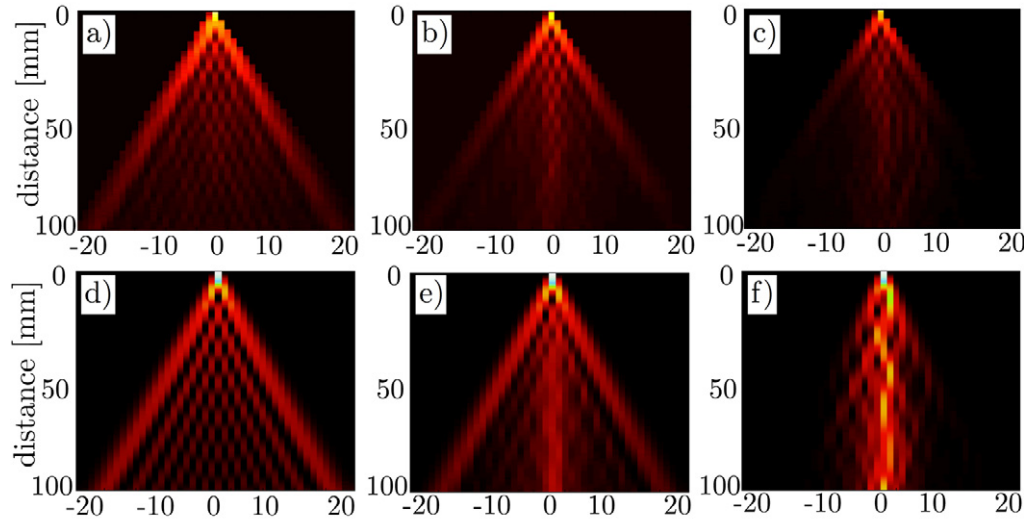
Figure 3. Averaged experimental fluorescence images (15 realizations) for different writing velocities: (a) ballistic spreading ($v_a = v_2 = 60 \, \text{mm} \, \text{min}^{-1}$), (b) superdiffusive behavior ($v_1 = 60 \, \text{mm} \, \text{min}^{-1}$, $v_2 = 67 \, \text{mm} \, \text{min}^{-1}$), (c) Anderson localization ($v_1 = 60 \, \text{mm} \, \text{min}^{-1}$, $v_2 = 75 \, \text{mm} \, \text{min}^{-1}$). Corresponding averaged simulations (100 realizations): (d) ballistic spreading $\Delta = 0$, (e) superdiffusive spreading $\Delta = C$ and (f) Anderson localization $\Delta = 4C$.

3. The experiment

In order to experimentally realize our RDM waveguide array, during the fabrication process we choose two different writing velocities v_1 or v_2 for each waveguide pair. This corresponds to a binary distribution ε_1 or ε_2 of the waveguide propagation constants. For reasons of simplicity, we fixed $v_1 = 60 \, \text{mm} \, \text{min}^{-1}$, and varied only v_2. Note that in all our experiments the difference in the writing velocities is sufficiently small to effectively not change the evanescent coupling between the guides, that is determined as $C_{\text{exp}} = 1.1 \, \text{cm}^{-1}$. Light transport in the waveguide arrays is analyzed using a fluorescence microscopy technique [26], where a light beam at $\lambda = 633 \, \text{nm}$ is launched into one of the two central lattice sites using a $10\times$ microscope objective. Five configurations of different values of Δ are investigated by controlling v_2. For each of the five Δ values, we prepare an array of 100 mm length consisting of 100 waveguides each, where each individual guide has a transverse dimension of $4 \times 11 \, \mu\text{m}$, and an average over 15 excitations of different waveguides is carried out to obtain $M(z)$. In figures 3(a)–(c) three examples of averaged experimental fluorescence intensity patterns are shown. From these diffraction patterns, we extract the variance of the spreading wavepacket. In figures 3(d)–(f) the corresponding simulations using equation (2) are plotted.

The measurements for $M(z)$ versus z are shown in figure 4(a) for five representative cases corresponding to $\Delta = 0$, $0 < \Delta < 2C$ and $\Delta > 2C$. Note the log–log-plot, allowing to directly extrapolate the slope to the spreading exponent. In the case of $v_1 = v_2 = 60 \, \text{mm} \, \text{min}^{-1}$, all waveguides are identical and hence we expect ballistic spreading of an initially localized wavepacket (blue line). A different transport regime is observed when we choose $v_2 = 65 \, \text{mm} \, \text{min}^{-1}$ (green line), $v_2 = 67 \, \text{mm} \, \text{min}^{-1}$ (red line) and $v_2 = 69 \, \text{mm} \, \text{min}^{-1}$ (yellow line), respectively. In these cases, we fulfill the condition of $\Delta < 2C$, resulting in the formation of

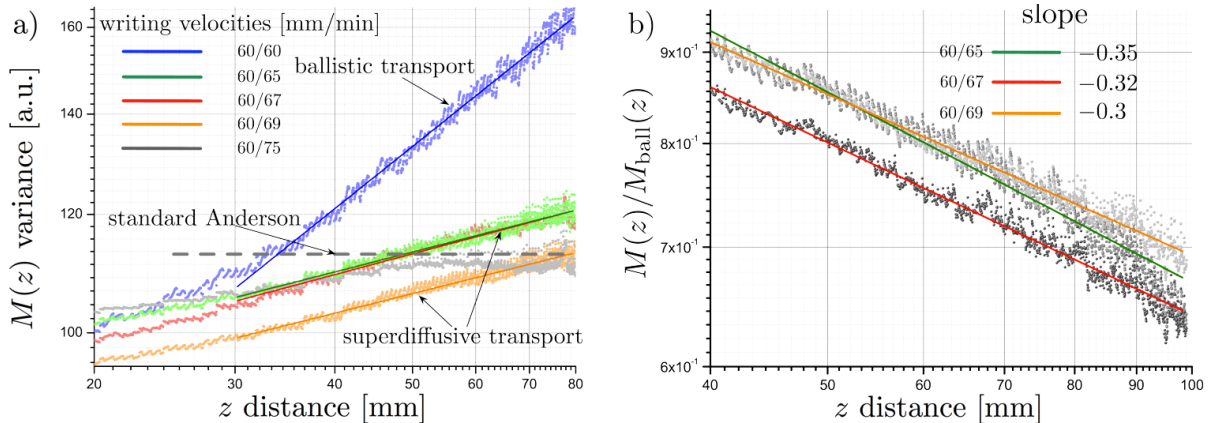**Figure 4.** (a) Directly extracted variances for various values of disorder Δ, as a function of the propagation distance. Note that in this log–log-plot, in the superdiffusive case, the slope of the variance is identical for the three different dimer configurations. (b) The ratio of the three variances in the superdiffusive regime and the ballistic variance in a double-logarithmic plot. The three graphs show a slope of $\approx -0.33 \pm 0.2$. Hence, taking into account the theoretical value of $\gamma_{\mathrm{ball}} = 2$, the diffusion exponent in the diffusive regime is $\gamma_{\mathrm{diff}} = 1.68 \pm 0.2$. This is very close to the predicted exponent of $\gamma_{\mathrm{theory}} = 1.5$ and, moreover, (almost) independent of the exact value of Δ.

extended near-resonance eigenmodes. The experimental data clearly shows that the slopes are identical (i.e. the spreading exponent is the same) but strongly reduced compared to the ballistic regime. Consequently, a spreading still occurs though it is sub-ballistic. Eventually, when we choose $v_2 = 75 \, \mathrm{mm \, min}^{-1}$, the disorder between the dimers is so strong that we enter the regime where $\Delta > 2C$, where one expects a full suppression of transport, i.e. Anderson localization. This is clearly shown in our experiments, as the width of the wavepacket (gray line in figure 4(a)) saturates with a vanishing spreading exponent $\gamma = 0$.

The directly extracted variance of the evolving wavepacket is significantly lower than the predicted behavior. This is mainly due to the existence of noise in the experiments that heavily affects the measured slope of the variance. Additionally, the fluorescence of the waveguides slightly decreases in time during the averaging process. However, we are able to calibrate our experimental results, by computing the ratio $M(z)/M_{\mathrm{ball}}(z) \sim z^\alpha$ where $M_{\mathrm{ball}}(z)$ is the experimentally measured spreading for the ballistic case. As both variances are equally affected by noise and bleaching, the measurement of the α-values allowed us to extract the spreading exponent $\gamma = \gamma_{\mathrm{ball}} + \alpha$ where $\gamma_{\mathrm{ball}} = 2$ as expected from equation (4), in the absence of noise and bleaching. The ratios of the measured variances are shown in figure 4(b). The green, red and yellow lines show the aforementioned ratio for the writing speeds $v_2 = 65 \, \mathrm{mm \, min}^{-1}$, $v_2 = 67 \, \mathrm{mm \, min}^{-1}$ and $v_2 = 69 \, \mathrm{mm \, min}^{-1}$, respectively, having respective slopes of -0.35, -0.32 and -0.3. We therefore find an experimental value for the spreading exponent in the superdiffusive regime of $\gamma_{\mathrm{diff}} = 1.68 \pm 0.2$ for these three configurations. This measured value is very close to the predicted exponent of $\gamma_{\mathrm{theory}} = 1.5$ associated with the superdiffusive spreading in our RDM. Additionally, as the model predicts, γ is (almost) independent of the exact value of Δ, as long as one has $0 < \Delta < 2C$.

In intuitive terms, we attribute the appearance of superdiffusion to the coexistence of the weak ballistic lobes and the central localized fraction of the wave. When computing the variance, the small but distant ballistic component has a significant effect, therefore resulting in the anomalous superdiffusive behavior of the wavepacket broadening.

4. Conclusion

In conclusion, we observed the transition between superdiffusive long-range transport and localization in a 1D random-dimer chain with short range-correlations between lattice sites. Below the transition, the transport is characterized by an anomalous (super-)diffusive spreading of the wave function. Our measurements were implemented in optical waveguide arrays, where the dynamics can be directly imaged from the top of the sample. We note that our findings are quite general and can apply to any physical setting where a RDM is applicable.

Acknowledgments

References

[1] Anderson P W 1958 *Phys. Rev.* **109** 1492
[2] Wiersma D S *et al* 1997 *Nature* **390** 671
[3] Cao H *et al* 1999 *Phys. Rev. Lett.* **82** 2278
    Cao H 2003 *Waves Random Media* **13** R1
[4] Chabanov A A, Stoytchev M and Genack A Z 2000 *Nature* **404** 850
[5] Pertsch T *et al* 2004 *Phys. Rev. Lett.* **93** 053901
[6] Störzer M *et al* 2006 *Phys. Rev. Lett.* **96** 063904
[7] Schwartz T, Bartal G, Fishman S and Segev M 2007 *Nature* **446** 525
[8] Lahini Y, Avidan A, Pozzi F, Sorel M, Morandotti R, Christodoulides D N and Silberberg Y 2008 *Phys. Rev. Lett.* **100** 013906
[9] Bodyfelt J *et al* 2009 *Phys. Rev. Lett.* **102** 253901
[10] Aspect A *et al* 2008 *Nature* **453** 891
[11] Roati G *et al* 2008 *Nature* **453** 895
[12] Hu H *et al* 2008 *Nature Phys.* **4** 945
[13] de Moura F, AB F and Lyra M L 1998 *Phys. Rev. Lett.* **81** 3735
    de Moura F, AB F, Santos M, NB Fulco U L, Lyra M L, Lazo E and Onell M E 2003 *Eur. Phys. J.* B **36** 81
    Schubert G, Weiße A and Fehske H 2005 *Physica* B **359–361** 801
[14] Izrailev F M, Krokhin A A and Makarov N M 2012 *Phys. Rep.* **512** 125
[15] Dunlap D H, Wu H-L and Phillips P W 1990 *Phys. Rev. Lett.* **65** 88
[16] Phillips P and Wu H L 1991 *Science* **252** 1805
[17] Schaff J-F, Akdeniz Z and Vignolo P 2010 *Phys. Rev.* A **81** 041604

[18] Bellani V *et al* 1999 *Phys. Rev. Lett.* **82** 2159
[19] Zhao Z *et al* 2007 *Phys. Rev.* B **75** 165117
[20] Luna-Acosta G A *et al* 2009 *Phys. Rev.* B **80** 115112
[21] Christodoulides D N, Lederer F and Silberberg Y 2003 *Nature* **424** 817
[22] Szameit A, Burghoff J, Pertsch T, Nolte S, Tuennermann A and Lederer F 2006 *Opt. Express.* **14** 6055
[23] Barthelemy P, Bertolotti J and Wiersma D S 2008 *Nature* **453** 495
[24] Itoh K, Watanabe W, Nolte S and Schaeffer C 2006 *MRS Bull.* **31** 620
[25] Szameit A and Nolte S 2010 *J. Phys. B: At. Mol. Opt. Phys.* **43** 163001
[26] Szameit A, Dreisow F, Hartung H, Nolte S, Tünnermann A and Lederer F 2007 *Appl. Phys. Lett.* **90** 241113
[27] Molina M I 1999 *Mod. Phys. Lett.* B **13** 837
[28] Kramer B and MacKinnon A 1993 *Rep. Prog. Phys.* **56** 1469
[29] Azbel M Ya 1983 *Phys. Rev.* B **28** 4106
[30] Izrailev F M, Kottos T and Tsironis G P 1995 *Phys. Rev.* B **52** 3274
      Bovier A 1992 *J. Phys. A: Math. Gen.* **25** 1021